[CANCER RESEARCH 62, 5139–5143, September 15, 2002]

Advances in Brief

Arginine-Glycine-Aspartic Acid (RGD)-Peptide Binds to Both Tumor and Tumor-Endothelial Cells *in Vivo*

Sabine Zitzmann, Volker Ehemann, and Manfred Schwab[1]

German Cancer Research Center, Department for Cytogenetics [S. Z., M. S.], and University of Heidelberg, Institute for Pathology, [V. E.], D-69120 Heidelberg, Germany

Abstract

Targeting tumor cells or tumor vasculature by peptides is a promising strategy for delivering cytotoxic drugs for cancer therapy. The identification of efficient targeting peptides depends on the availability of informative methods for determining cellular binding specificities. Here, we have used fluorescence-activated cell-sorting (FACS) analysis in combination with an isopentane freezing method to show targeted binding of the Arg-Gly-Asp (RGD)-4C-peptide labeled with FITC, not only to endothelial cells but also to tumor cells in human breast cancer xenografts grown in nude mice. Nontumorous cells showed only background binding. This study suggests, that the RGD-4C-peptide can target tumor endothelial cells as well as tumor cells. Consequently, it should be possible to design a combination therapy approach against both targets.

Introduction

Targeting drugs to tumor cells is a central challenge for improving existing cancer therapies. Directing therapeutic agents, like chemo- or radiotherapeutic drugs, viruses for gene therapy, enzymes for prodrug therapy, or toxins, to the tumor cells or tumor blood vessels is likely to enhance the efficacy of anticancer drugs and to decrease side effects (1). Different strategies have been pursued to achieve this goal. The most commonly used vehicles for tumor targeting are "engineered antibodies," *i.e.*, bispecific antibodies or antibody fragments (2–4). "Homing" peptides are promising alternatives, because they bind to surface molecules specific to organ or tumor cells (5–7) but are smaller than the antibody fragments.

Phage display techniques have been a productive instrument toward identifying peptides for targeting organs, tumors, or cell types (8). Present data obtained from phages expressing the homing peptide on their surface suggest that the endothelial lining of the blood vessels of tumors is the primary target for peptides (9). A prominent example for a homing peptide is the three-amino-acid sequence RGD[2] motif (10, 11). It is present in many extracellular matrix components such as fibronectin and vitronectin and binds to integrins. RGD-analogues are used in tumor imaging (12), in antiangiogenesis approaches (13), and in tumor targeting with radionucleotides (14) or chemotherapeutic drugs (6).

Demonstrating *in vivo* targeting of peptides to particular cell types or organs is subject to a number of limitations, mainly because currently used technologies, such as the localization of radiolabeled peptides by positron emission tomography (PET) or by a gamma counter, produces only an imprecise picture. Using phages instead that display the peptides on their surface has other restrictions, particularly because phages are taken up by the reticuloendothelial system (RES; Ref. 15) and unspecifically bind to liver, kidney, and spleen (5).

Here, we present an analysis of the *in vivo* binding specificity of the RGD-4C-peptide (6) by FACS measurements. Suspensions of intact cells were prepared by using a combination of isopentane freezing (16) and a cell strainer. We show that the FITC-labeled peptide is able to bind to both tumor cells and endothelial cells, whereas only background binding was seen for cells of various other organs. Our results suggest that both the tumor endothelial cells and the tumor cells provide potential targets for cancer therapy.

Materials and Methods

Animals. Female 6-week-old BALB/c *nu/nu* mice were obtained from Charles River (Sulzfeld, Germany) and housed in VentiRacks.

Peptide. RGD-4C-Peptide was synthesized by Synthem (Nimes, France) with the sequence CDCRGDCFC (10) and was coupled to FITC.

Cell Line. MDA-MB 435 breast carcinoma was kindly provided by Dr. Iduna Fichtner (Berlin, Germany). The cells were cultured in RPMI 1640 containing 10% FCS in a 5% CO_2-incubator at 37°C.

Tumor Targeting. MDA-MB 435 cells were grown to 90% confluency, harvested with PBS/EDTA (10 mM), resuspended in Matrigel-Matrix (FALCON) and kept on ice. Two hundred μl of the Matrigel-Matrix/cell suspension (5×10^6 cells) were injected s.c. into the anterior region of the mouse trunk. Tumors were grown to a size of ~1.0 cm^3. One hundred μg of RGD-4C-FITC-peptide were injected into the tail vein of the mouse. The mice were anesthetized with 5 mg of Ketanest (Parke-Davis, Berlin, Germany) and 400 μl of 0.2% Rompun (BayerVital, Leverkusen, Germany) were injected i.p. Under full anesthesia, the mice were perfused through the heart with 25 ml 0.9% NaCl, and tumor and control organs were removed and snap-frozen in isopentane cooled with liquid nitrogen and were stored at −80°C.

Single-Cell Suspension Preparation. The frozen tissue was thawed on ice. A cell strainer (FALCON) was placed on top of a 50-ml Falcon tube, the tissue was placed into the strainer, and ~0.5 ml of PBS was added. Gentle pressure was applied, and the tissue was squeezed through the cell strainer, which resulted in a single-cell suspension. More PBS was added to rinse the cell strainer up to a total volume of ~4 ml. Depending on the cell density, 50–100 μl of this suspension were added to a DAPI solution (25 μg/ml in PBS) and used for FACS analysis.

FACS Analysis. FACS analysis was done in a Galaxy Pro flow cytometer (Partec, Münster, Germany) equipped with a mercury vapor lamp (100 W) and filter combinations for DAPI and a 488-nm argon laser with filter combination for FITC. Histogram and dot blot analysis was done with the Flowmax analysis software (Partec).

To discriminate between peptide-bound labeled cells and autofluorescence of unlabeled cells, the autofluorescence of tumor and control organ cells was measured. A cutoff point was determined at which more than 95% of the unlabeled cells were below a defined value (mean of 4 independently experiments); this value was defined as the cutoff-line. Fluorescence up to this intensity was considered as autofluorescence and all of the cells in which fluorescence was higher than the cutoff value were considered as labeled by RGD-4C-FITC-peptide.

Immunostaining for FACS Analysis. The R-PE-conjugated rat antimouse CD31 (PECAM-1) monoclonal antibody against endothelial cells was obtained from PharMingen Europe. Tumors single-cell suspensions were prepared from fresh tumor tissue as described above. The PECAM-1 antibody was used in a

Received 1/29/02; accepted 8/2/02.

The costs of publication of this article were defrayed in part by the payment of page charges. This article must therefore be hereby marked *advertisement* in accordance with 18 U.S.C. Section 1734 solely to indicate this fact.

[1] To whom requests for reprints should be addressed, at German Cancer Research Center, Department for Cytogenetics H0400, Im Neuenheimer Feld 280, D-69120 Heidelberg, Germany. E-mail: m.schwab@dkfz.de.

[2] The abbreviations used are: RGD, Arg-Gly-Asp; FACS, fluorescence-activated cell sorting; DAPI, 4′,6-diamidino-2-phenylindole; PE, phycoerythrin; D.I., DNA index.

1:10 dilution, and 100 μl of single-cell suspension were incubated with the antibody for 30 min at room temperature. The cells were washed with FACS buffer before FACS measurements.

Results

Determination of RGD-4C-Peptide Binding *in Vivo* by FACS Analysis. We have studied the distribution of the CDCRGDCDC peptide coupled with FITC (RGD-4C-FITC-peptide) after i.v. injection into tumor-bearing nude mice. MDA-MB 435 human breast cancer xenografts (diameter, 1–1.5 cm) were used as the target. RGD-4C-FITC-peptide was injected into the tail vein of the mice and allowed to circulate in the blood stream for various time periods ranging from 5 min to 2 h. Subsequently, the mice were perfused with 0.9% NaCl to remove blood and unbound peptide. The tumor and control organs were excised and snap-frozen in isopentane cooled with liquid nitrogen. For FACS measurements, the tissue was gently squeezed through a cell strainer. The single cells suspension was then stained with DAPI for analysis of the DNA content.

Forward and sideward scatter diagrams of single-cell solutions prepared from tumor and control organs, as well as microscopic inspections of cell preparations, demonstrated that at least the majority of cells was still intact with only small amounts of debris (Figs. 1 and 2). The single-cell suspensions obtained from various organs showed their organ-characteristic cell cycle distribution, as determined by DAPI stain. For instance, liver DNA histograms showed cells with tetraploid and octoploid DNA status. In spleen, a large proportion of cells were in S phase, whereas in kidney, most cells were in G_0-G_1, few cells were in G_2-M, and S-phase cells were almost absent.

Tumor-derived and control organ cells from mice that had received injections with RGD-4C-FITC-peptide showed a higher FITC-fluorescence (Fig. 3) than did the corresponding cells from control mice. This was not seen with FITC alone (data not shown). To discriminate between fluorescence caused by peptide binding and autofluorescence of unlabeled cells, the autofluorescence of tumor-derived cells and of control organ cells was measured, and a cutoff point was determined

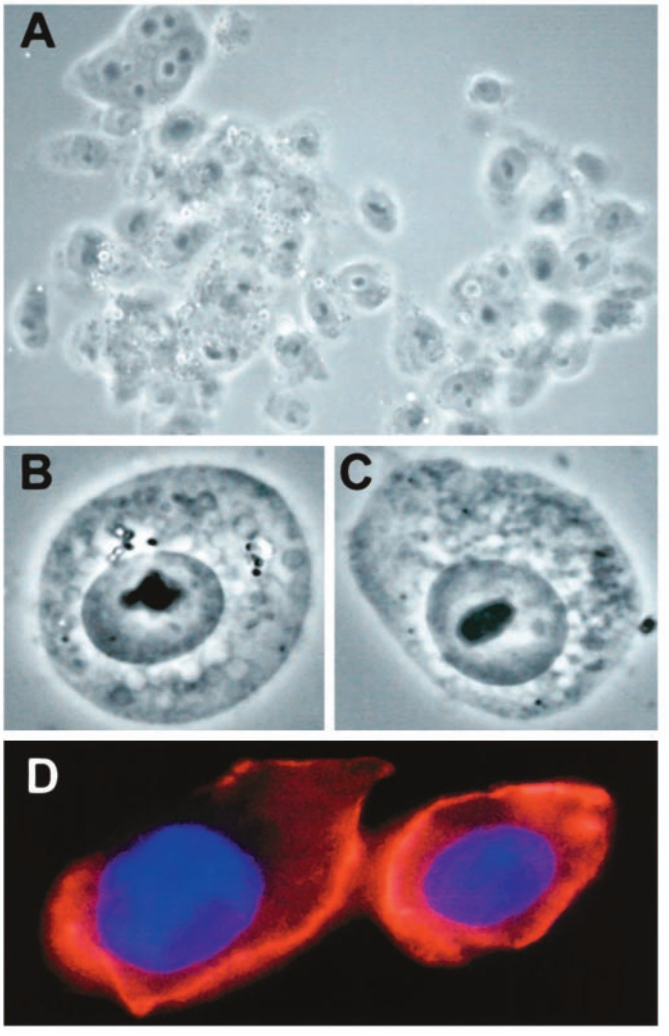

Fig. 2. Single-cell suspension obtained from MDA-MB 435 breast cancer cells grown in nude mice. The mice were sacrificed and perfused, and the tumor was snap-frozen in isopentane. The tumor was thawed and squeezed through a cell strainer. *A–C*, the cells fresh from the preparation in phase contrast (*A*, ×200; *B* and *C*, ×630). *D*, the cells from the same cell preparation stained with DAPI for DNA and cell-membrane labeling with 50 μg/ml wheat-germ agglutinin coupled with biotin (Pierce) for 30 min. Detection was performed with 5 μg/ml Streptavidin-PE (PharMingen).

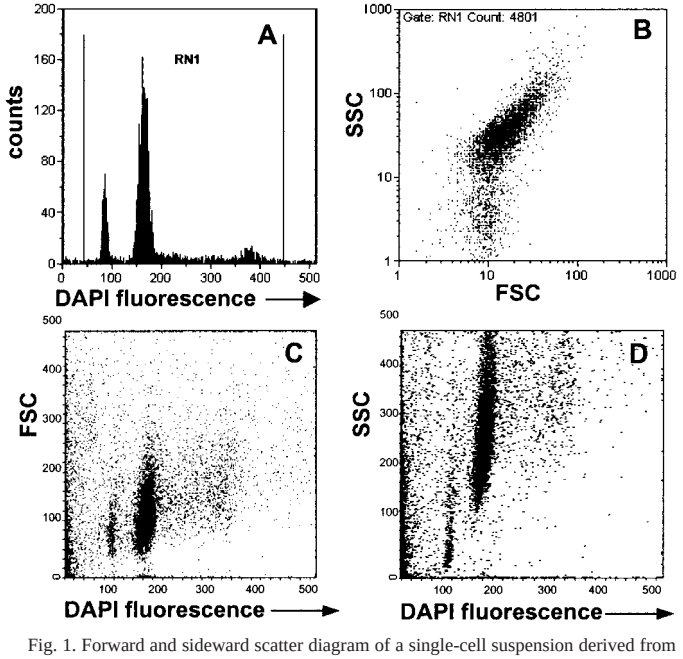

Fig. 1. Forward and sideward scatter diagram of a single-cell suspension derived from a tumor with the corresponding DAPI-stain diagrams. Tumor was grown in BALB/c *nu/nu* mice, removed after perfusion, and frozen in isopentane cooled with liquid nitrogen. After thawing, the tumor was squeezed through a cell strainer, and the single-cell suspension obtained was stained with DAPI and measured with FACS analysis.

(experimental protocol; Fig. 4*D*). The RGD-4C-FITC-peptide accumulated preferentially in the tumor-derived cells within 5 min after injection (Fig. 5*A*). More than 60% of the cells obtained from the tumor were labeled with the RGD-4C-FITC-peptide, a level that remained stable for more than 30 min. Both the 5-min and 30-min time points showed a significantly higher FITC-fluorescence for tumor-derived cells than for liver cells, which demonstrated the tumor specificity of the RGD-4C-FITC-peptide. Highly significant was the difference between tumor and liver at the 5-min time point ($P = 0.0259$). After 30 min, an overall decrease in FITC-fluorescence was observed. One hundred twenty min after RGD-4C-FITC-peptide injection, FITC-fluorescence had assumed the background level in both the tumor and control organs. The liver cells showed a slower and lower accumulation of the peptide than did the tumor cells but a similar decrease of RGD-4C-FITC-peptide after 30 min. In contrast to tumor and liver cells, spleen and kidney cells showed rapidly accumulated RGD-4C-FITC-peptide within the first 5 min after injection; however, the fluorescence intensity decreased rapidly and reverted to background level after 30 min. To demonstrate that the binding is specific and not caused by the presence of just any peptide, the same

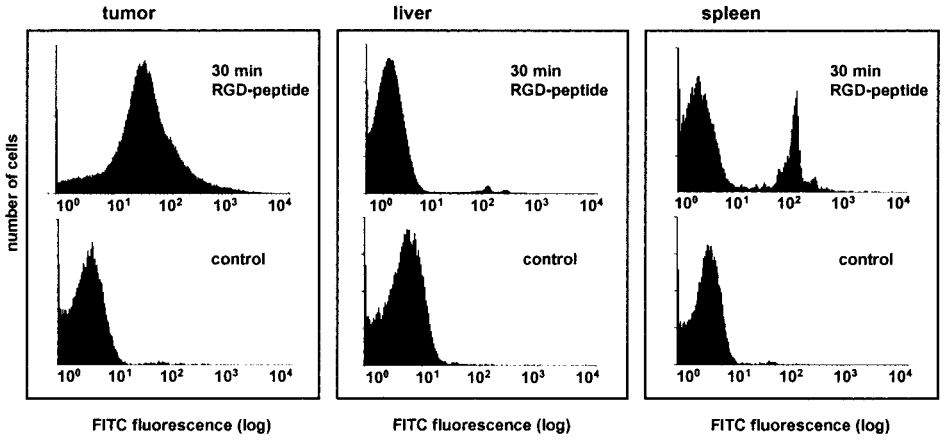

Fig. 3. Flow-cytometry demonstrating the binding of RGD-FITC-labeled peptide to cells of different organs in BALB/c *nu/nu* mice. The RGD-FITC-labeled peptide was injected into the tail vein of mice. Mice were sacrificed after 30 min, and they were perfused through the heart with 25 ml of 0.9% NaCl tissues were isolated and frozen in isopentane. After preparing single-cell suspension with a cell strainer, the cells were measured with FACS analysis for FITC fluorescence. Control cells were taken from experiments without peptide injection. Instrumental setting of the Galaxy Pro during experimental measurement and the control measurement were identical.

experiments were conducted with the FITC-labeled peptide VPWME-PAYQRFL as controls. No FITC-labeling of the tumor cells was observed (data not shown).

RGD-4C Binds to Tumor Cells and to Tumor Endothelial Cells *in Vivo*. To determine the target cells of RGD-4C-FITC-peptide binding within the xenograft, the single-cells suspension derived from the MDA-MB 435 was stained with DAPI. Forward and sideward scatter by FACS determined two separate cell populations with different size and granularity (Fig. 1). DAPI measurements identified one cell population with a D.I. of 0.894 and another population with a D.I. of 1.31, in reference to human lymphocytes (17).

Comparison with cells from various mouse organs identified the cells with the lower D.I. as of mouse origin. To further characterize the mouse cells in the tumor-derived single-cell solution, we used the endothelial-specific antibody PECAM-1. A positive reaction was seen with the mouse cells, whereas it did not stain the tumor cells (Fig. 6), which suggested that at least the major portion of the mouse cells in the tumor-derived cell suspension consisted of endothelial cells. An isotype-matched control antibody did not stain either the endothelial cells or the tumor cells (Fig. 6*C*). To determine the affinity of the two cell populations to the RGD-4C-FITC-peptide, the single-cell suspen-

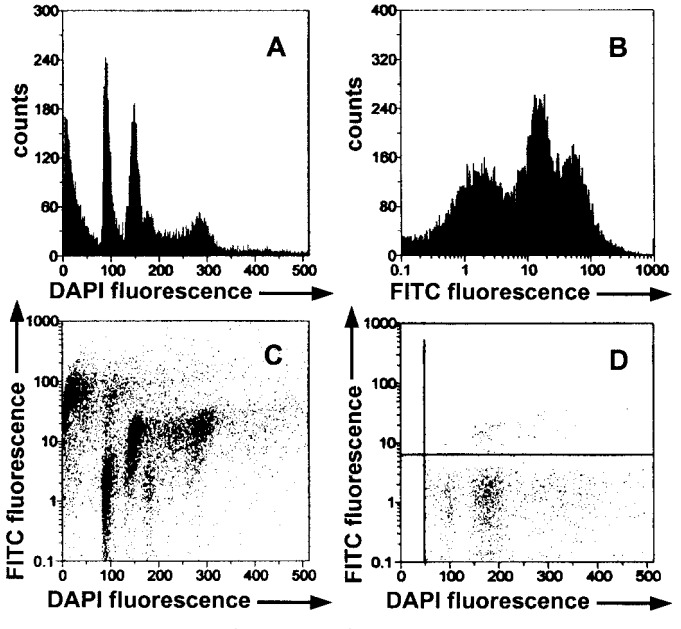

Fig. 4. FACS histograms of cells derived from MDA-MB 435 tumors grown in nude mice. RGD-FITC-peptide (100 μg) was injected into the tail vein of the mouse (*A–C*) and was allowed to circulate for 15 min. *D*, a control; no peptide has been injected, and cells show only autofluorescence. Cells were prepared with a cell strainer and stained with DAPI. (*A*) DAPI stain for cell cycle (*B*) FITC-fluorescence of the tumor-derived cells (*C*) DAPI stain *versus* FITC fluorescence to show cell type-specific labeling (*D*) control (no RGD-FITC-peptide was injected) DAPI stain *versus* FITC fluorescence showing the cutoff that has been used to determine the percentage of labeled cells.

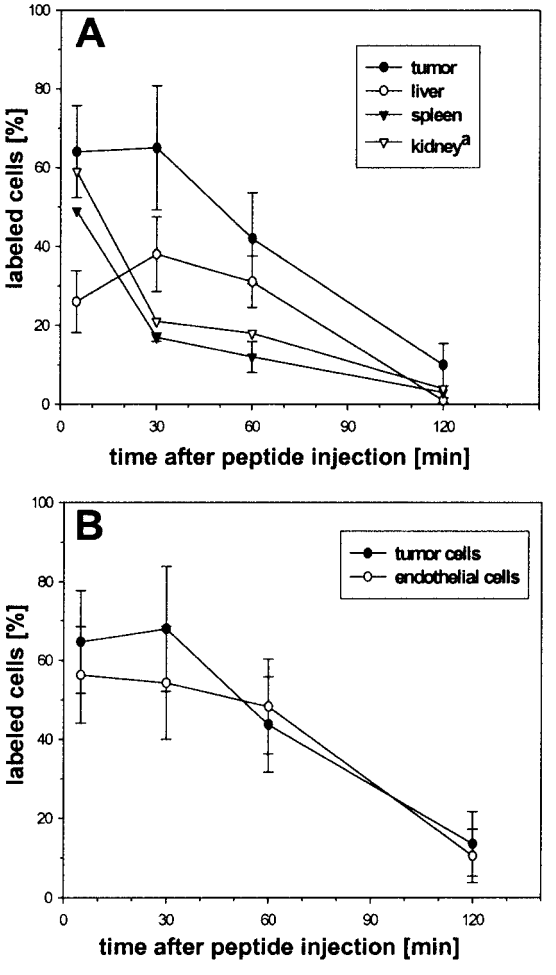

Fig. 5. RGD-FITC-peptide (100 μg) was injected into the tail vein of mice bearing MDA-MB 435 breast-carcinoma tumors (~1 cm in diameter). After the indicated time points the mice were sacrificed, samples were taken, and FITC fluorescence was measured by FACS. *A*, the percentage of labeled cells (fluorescence value of cells was more than the cutoff determined with control cells) for tumor-derived cells and various control organs and the SE from three independent sets of experiments (*kidney*, data resulted from one experiment). *B*, the percentage of labeled cells (the fluorescence value of the cells is more than the cutoff value determined with control cells) for tumor cells and endothelial cells and the SE from three independent sets of experiments. The percentage of labeled cells is calculated for 100% of the cells from each population.

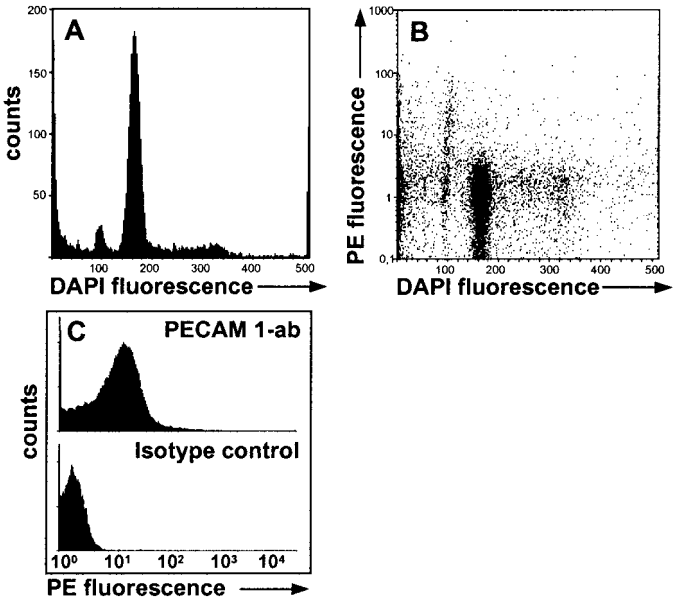

Fig. 6. FACS histograms of cells derived from MDA-MB 435 tumors grown in nude mice. Cells were prepared with a cell strainer and stained with DAPI and PE-conjugated rat antimouse CD31 (PECAM-1) monoclonal antibody against endothelial cells for 30 min. (A) DAPI stain for cell cycle (B) DAPI stain *versus* PE-PECAM fluorescence for endothelial cell labeling (C) An isotype-matched control antibody did not stain neither the endothelial cells nor the tumor cells.

sion was stained with DAPI and analyzed by FACS for cell cycle and FITC fluorescence. Both cell populations bound the RGD-4C-FITC-peptide with similar efficiency (Fig. 5*B*). In both populations, about 60% of the cells were FITC labeled within 5 min after injection. This level remained stable for ~30 min; subsequently, the fluorescence intensity decreased to background level after 2 h. No significant difference in binding between mouse endothelial cells and tumor cells was observed at any time point.

Our results suggest that the RGD-4C-FITC-peptide binds to both endothelial and tumor cells *in vivo* and that peptide targeting should allow the delivery of therapeutic drugs to both endothelial and tumor cells.

Discussion

The main conclusion that we draw from the present study is that the RGD-4C-peptide is capable of targeting coupled molecules not only to endothelial cells but also to the tumor cells of human xenografts. Experimentally, this result was achieved by a suitable combination of cell preparation with FACS analysis. First, the sample preparation is an important step in which we have used isopentane freezing of total tissue, which resulted in fully preserved cells (16, 18). Second, FACS analysis proved to be an informative tool to show RGD-4C-FITC-peptide binding to both mouse endothelial and human tumor cells.

The RGD-4C-peptide was used in this study because it is a promising candidate for both tumor therapy and tumor imaging. For instance, a cyclic RGD-peptide has been shown to inhibit the growth of human melanoma xenografts in nude mice (19). Furthermore, radiolabeled cyclic RGD-peptides have demonstrated specificity for xenograft tumors expressing $\alpha_V\beta_3$ integrins (20). A more detailed analysis of RGD-peptide binding within the tumor has been missing thus far, because of the unavailability of an informative assay.

MDA-MB 435 cells express RGD-receptors, α_V integrins, on their surface (21, 22), and the receptor is also up-regulated in angiogenic endothelial cells (23). Despite this, previous studies, using bacteriophages displaying the RGD-4C-peptide that was fused to a surface protein and that was introduced into the blood stream of mice carrying MDA-MB 435 xenografts, had shown that the RGD-4C-phages attached exclusively to endothelial cells, not to tumor cells (10). This seemingly contradictory result may be best explained by the size difference between the peptide displaying bacteriophage and the peptide FITC conjugate. It is known that blood vessels in tumor have an increased vascular leakiness, as compared with vessels of normal tissue (24, 25), and the RGD-4C-FITC complex may be sufficiently small to penetrate into the tumor tissue through the endothelial vessel lining. The display phages, in contrast, might be too large. Binding of the peptide during sample preparation appears to be an unlikely possibility, because the mice were perfused through the heart, and the major portion of blood and unbound peptide was washed out before removing the tumor and control organs.

The very rapid enrichment of the RGD-FITC-peptide and its consistent high level both in tumor and in endothelial cells for 30 min is a good indicator for peptide specificity. The liver is slower to accumulate the peptide, and the level of peptide binding is lower than in the tumor. This observation is supported by a study using a ^{18}F-labeled RGD-containing glycopeptide and positron emission tomography (12), which showed preferential binding to $\alpha_v\beta_3$-integrin-expressing tumors in comparison with $\alpha_v\beta_3$-integrin-negative tumors. In line with the observation in this present study, the peptide also showed a rapid renal excretion, which indicated rapid blood clearance of the peptide. These observations seem to be consistent with those in patients during imaging with a technetium-99m-labeled RGD-peptide (26), during which rapid serum clearance via the kidney within several minutes after peptide application was seen.

The suitability of peptide targeting to tumor cells is supported by a recent study of FITC-labeled peptides binding to human head and neck tumor xenografts and to *in vitro* cultivated cells (7). *In vivo*, the cells of the human xenografts accumulated fluorescence signals after injection of the FITC-labeled peptide into the blood stream of the mice. *In vitro*, FITC-labeled peptides became internalized into the tumor cells. These observations differ from our own results, in which we were unable to detect FITC-labeled RGD-4C-peptides by fluorescence microscopy. A potential explanation is that the internalized head and neck tumor peptide accumulates to form readily detectable structures, whereas the RGD-FITC-peptide is not internalized; and it is probable that the signal from scattered FITC molecules is not sufficiently strong to be detected microscopically. The discrimination of endothelial cells and tumor cells should be feasible in most animal models and will allow a more detailed assessment of the peptide-binding specificity within the tumor. In sum, our observation of efficient RGD-FITC-peptide binding both to endothelial and to tumor cells raises the possibility of designing combination therapies directed against both targets that could be more efficient than the single-target therapeutic regimens alone.

References

1. Jain, R. K. The next frontier of molecular medicine: delivery of therapeutics. Nat. Med., *4:* 655–657, 1998.
2. Chames, P., and Baty, D. Antibody engineering and its applications in tumor targeting and intracellular immunization. FEMS Microbiol. Lett., *189:* 1–8, 2000.
3. Hudson, P. J. Recombinant antibody constructs in cancer therapy. Curr. Opin. Immunol., *11:* 548–557, 1999.
4. DeNardo, S. J., Kroger, L. A., and DeNardo, G. L. A new era for radiolabeled antibodies in cancer? Curr. Opin. Immunol., *11:* 563–569, 1999.
5. Pasqualini, R., and Ruoslahti, E. Organ targeting *in vivo* using phage display peptide libraries. Nature (Lond.), *380:* 364–366, 1996.
6. Arap, W., Pasqualini, R., and Ruoslahti, E. Cancer treatment by targeted drug delivery to tumor vasculature in a mouse model. Science (Wash. DC), *279:* 377–380, 1998.
7. Hong, F. D., and Clayman, G. L. Isolation of a peptide for targeted drug delivery into human head and neck solid tumors. Cancer Res., *60:* 6551–6556, 2000.
8. Mazzucchelli, L., Burritt, J. B., Jesaitis, A. J., Nusrat, A., Liang, T. W., Gewirtz, A. T., Schnell, F. J., and Parkos, C. A. Cell-specific peptide binding by human neutrophils. Blood, *93:* 1738–1748, 1999.

9. Pasqualini, R. Vascular targeting with phage peptide libraries. Q. J. Nucl. Med., *43:* 159–162, 1999.
10. Pasqualini, R., Koivunen, E., and Ruoslahti, E. α_v integrins as receptors for tumor targeting by circulating ligands. Nat. Biotechnol., *15:* 542–546, 1997.
11. Ruoslahti, E. RGD and other recognition sequences for integrins. Annu. Rev. Cell Dev. Biol., *12:* 697–715, 1996.
12. Haubner, R., Wester, H. J., Weber, W. A., Mang, C., Ziegler, S. I., Goodman, S. L., Senekowitsch-Schmidtke, R., Kessler, H., and Schwaiger, M. Noninvasive imaging of $\alpha_v\beta_3$ integrin expression using 18F-labeled RGD-containing glycopeptide and positron emission tomography. Cancer Res., *61:* 1781–1785, 2001.
13. Pasqualini, R., Koivunen, E., Kain, R., Lahdenranta, J., Sakamoto, M., Stryhn, A., Ashmun, R. A., Shapiro, L. H., Arap, W., and Ruoslahti, E. Aminopeptidase N is a receptor for tumor-homing peptides and a target for inhibiting angiogenesis. Cancer Res., *60:* 722–727, 2000.
14. van Hagen, P. M., Breeman, W. A., Bernard, H. F., Schaar, M., Mooij, C. M., Srinivasan, A., Schmidt, M. A., Krenning, E. P., and de Jong, M. Evaluation of a radiolabelled cyclic DTPA-RGD analogue for tumour imaging and radionuclide therapy. Int. J. Cancer, *90:* 186–198, 2000.
15. Geier, M. R., Trigg, M. E., and Merril, C. R. Fate of bacteriophage lambda in non-immune germ-free mice. Nature (Lond.), *246:* 221–223, 1973.
16. Jehl, B., Bauer, R., Dorge, A., and Rick, R. The use of propane/isopentane mixtures for rapid freezing of biological specimens. J. Microsc., *123:* 307–309, 1981.
17. Melamed, M. R., Lindmo, T., Mendelsohn, M. L. Flow Cytometry and Sorting, 2nd Ed. New York: Wiley Publishers, 1990.
18. McGinley, D. M., Posalaky, Z., and Posalaky, I. P. The use of fresh-frozen tissue in diagnostic transmission electron microscopy. Ultrastruct. Pathol., *6:* 89–98, 1984.
19. Mitjans, F., Meyer, T., Fittschen, C., Goodman, S., Jonczyk, A., Marshall, J. F., Reyes, G., and Piulats, J. *In vivo* therapy of malignant melanoma by means of antagonists of α_v integrins. Int. J. Cancer, *87:* 716–723, 2000.
20. Haubner, R., Wester, H. J., Reuning, U., Senekowitsch-Schmidtke, R., Diefenbach, B., Kessler, H., Stocklin, G., and Schwaiger, M. Radiolabeled $\alpha_v\beta_3$ integrin antagonists: a new class of tracers for tumor targeting. J. Nucl. Med., *40:* 1061–1071, 1999.
21. Zhou, Q., Sherwin, R. P., Parrish, C., Richters, V., Groshen, S. G., Tsao-Wei, D., and Markland, F. S. Contortrostatin, a dimeric disintegrin from Agkistrodon contortrix contortrix, inhibits breast cancer progression. Breast Cancer Res. Treat., *61:* 249–260, 2000.
22. Wong, N. C., Mueller, B. M., Barbas, C. F., Ruminski, P., Quaranta, V., Lin, E. C., and Smith, J. W. α_v integrins mediate adhesion and migration of breast carcinoma cell lines. Clin. Exp. Metastasis, *16:* 50–61, 1998.
23. Ruoslahti, E., and Engvall, E. Integrins and vascular extracellular matrix assembly. J. Clin. Investig., *99:* 1149–1152, 1997.
24. Dvorak, H. F., Nagy, J. A., and Dvorak, A. M. Structure of solid tumors and their vasculature: implications for therapy with monoclonal antibodies. Cancer Cells, *3:* 77–85, 1991.
25. Plate, K. H., Breier, G., and Risau, W. Molecular mechanisms of developmental and tumor angiogenesis. Brain Pathol., *4:* 207–218, 1994.
26. Sivolapenko, G. B., Skarlos, D., Pectasides, D., Stathopoulou, E., Milonakis, A., Sirmalis, G., Stuttle, A., Courtenay-Luck, N. S., Konstantinides, K., and Epenetos, A. A. Imaging of metastatic melanoma utilising a technetium-99m labelled RGD-containing synthetic peptide. Eur. J. Nucl. Med., *25:* 1383–1389, 1998.